Limited iron isotope variation among tissues of a marine fish: a case study of wild chub mackerel (*Scomber japonicus*)

Nanako Hasegawa*[1,2], Yoshio Takahashi[1], Takaaki Itai[1]

[1]Department of Earth and Planetary Science, The University of Tokyo, 7-3-1 Hongo, Bunkyo-ku, 8 Tokyo 113-0033, Japan
[2]Faculty of Veterinary Medicine, Hokkaido University, Kita 18, Nishi 9, Kita-ku, Sapporo 060-0818, Hokkaido Japan.

Correspondence to: Nanako Hasegawa (n-hasegawa@vetmed.hokudai.ac.jp)

Abstract

Iron homeostasis in marine organisms operates under chronically low iron bioavailability, which may shape the strategies of iron uptake and storage in fish. Stable iron isotope ratios (δ^{56}Fe) have emerged as tracers of iron storage and uptake in terrestrial mammals, yet the physiological drivers of isotope fractionation in marine organisms remain poorly understood. Here, we investigated δ^{56}Fe variation and iron speciation across eight tissues of wild chub mackerel (*Scomber japonicus*), along with pool size estimation of key Fe species, including ferritin-bound (ferric) and heme-bound (mainly ferrous) Fe, using Fe K-edge X-ray Absorption Near Edge Structure (XANES) spectroscopy. In all the specimens, the liver δ^{56}Fe values were higher than the average value of all tissues, with an apparent isotopic shift between ferritin- and heme-bound Fe (Δ^{56}Fe) in the liver averaging 2.72 ± 3.03‰ (2 S.D.). In contrast to the liver, no enrichment of heavy Fe isotope was observed in the ovary and red muscle despite their high ferritin-Fe contribution, suggesting a high interconversion rate between ferritin- and heme-bound Fe pools in these tissues. The overall range of δ^{56}Fe variation among tissues was smaller than that reported in mammals. Our results suggested that muscular δ^{56}Fe in marine teleost is primarily governed by source signatures and intestinal uptake efficiency, while tissue heterogeneity due to heavy Fe storage by ferritin exerts only a minor influence. These findings highlight the potential of δ^{56}Fe as a proxy for intestinal iron acquisition in fish and provide new geochemical perspectives on iron cycling through marine food webs.

Short summary

Iron stable isotope ratios provide a potential tracer of iron metabolism in fish. Here, we report tissue-specific isotope variations in mackerel and evaluate how storage iron as ferritin affects fractionation using speciation analysis. The results show small isotopic differences among tissues, indicating that isotope ratios are primarily controlled by dietary values and intestinal uptake, highlighting the potential of natural isotope patterns as physiological indicators in fish.

1 Introduction

Iron is an essential element for life, functioning in electron transfer through the redox cycling between Fe^{2+} and Fe^{3+} (Georgiadis et al., 1992; Hoffbrand et al., 1976; Robbins and Pederson, 1970). While soluble Fe^{2+} is highly bioavailable, insoluble Fe^{3+} dominates under atmospheric conditions (Crichton and Boelaert, 2001), resulting in dissolved iron concentrations below 2 nmol L^{-1} in the open ocean (Hatta et al., 2015; Johnson et al., 1997; Martin and Gordon, 1988; Nishioka and Obata, 2017). This scarcity constitutes a major factor limiting primary production by phytoplankton (Boyd et al., 2000; Martin et al., 1989; Martin and Gordon, 1988).

Although iron limitation in primary producers is well established, its implications for higher organisms such as fish remain less understood. Unlike phytoplankton, tissue iron concentrations in fish are not directly constrained by seawater iron availability (Galbraith et al., 2019). This is based on long-term iron retention strategies via ferritin (iron storage protein) and efficient intestinal absorption mechanisms that specifically exist in marine fish (Bury et al., 2001; Carriquiriborde et al., 2004; Kwong and Niyogi, 2008). However, direct quantification of intestinal iron uptake has been largely restricted to laboratory animals using enriched isotopes (van den Heuvel et al., 1998, Fiorio et al., 2012), an approach that is not feasible for wild species especially marine fish.

Natural iron stable isotope ratios (δ^{56}Fe) offer a broadly applicable, non-lethal proxy for assessing iron metabolism. δ^{56}Fe values are sensitive to intestinal absorption processes (Albalat et al., 2021; Flórez et al., 2017; Van Heghe et al., 2013; Hotz and Walczyk, 2013; Krayenbuehl et al., 2005; Stenberg et al., 2003) as well as to variation in iron storage and homeostasis, with ferritin-bound iron often implicated as a key driver of tissue-specific fractionation in mammals (Van Heghe et al., 2014; Hotz et al., 2012; Jaouen and Balter, 2014). Extending this framework to fish requires evaluating both intestinal absorption and ferritin-associated storage effects.

In this study, we examined δ^{56}Fe distributions across tissues of marine fish chub mackerel (*Scomber japonicus*). Additionally, X-ray Absorption Near-edge Structure (XANES) spectroscopy provided a non-destructive and oxidation state–sensitive approach to quantify ferritin-bound iron, allowing direct estimation of the proportion of Fe^{3+} species in tissues without chemical extraction. Using this method, we quantified the relative contributions of ferritin- and heme-bound iron and assessed their roles in isotopic variability. By further considering physiological factors such as sex and reproductive status, our study provides new insights into the mechanisms governing δ^{56}Fe fractionation in fish and its potential as a tracer of intestinal iron acquisition in marine ecosystems.

2 Materials and Method

2.1 Sample Collection and Preparation

Six adult chub mackerel (females: Mk-1 to Mk-3, males: Mk-4 to Mk-6) were collected by longline fishing around Tsushima Island, East China Sea, on April 27, 2022. Fish were frozen onboard at −30 ℃, stored at −20 to −25 ℃ for eight

60 days, and subsequently transported to the laboratory at −15 ℃. Body weight and fork length were recorded prior to dissection. Total blood volume was estimated as 60 mL/kg according to teleost values (Brill et al., 1998; Itazawa et al., 1983). Each individual was dissected into eight tissues (red and white muscle, liver, gonad, spleen, heart, gills, and blood). All tissue samples were stored at −80℃ until the analysis. Wet weight was measured, and hepatosomatic index (HSI) and gonadosomatic index (GSI) were calculated as follows (Allaya et al., 2013; Shiraishi et al., 2008):

65 $$HSI = \frac{Liver\ weight}{Total\ body\ weight} \times 100 \quad (1)$$

$$GSI = \frac{Gonad\ weight}{Somatic\ weight} \times 100 \quad (2)$$

Tissues with high iron content (red muscle, liver, gonad, blood, and heart) were selected for Fe K-edge XANES analysis. Small frozen fragments were immediately sealed in oxygen-impermeable polycarbonate film (ASONE, Japan) after dissection and stored until measurement.

70

2.2 Iron Concentration and Stable Isotope Measurement

Analytical procedures followed by Hasegawa et al., (2023). Tissues were freeze-dried, and lipids removed from liver and gonad using chloroform:methanol mixture (2:1, v/v). Tests with certified reference materials confirmed no significant isotopic alteration during lipid removal (<0.07‰, n=4). Dried tissues (0.3–2.5 g) were digested in perfluoroalkoxy (PFA) vials
75 using 68% HNO_3 and 35% H_2O_2 (both Tamapure AA-100, Tama Chemical Corp., Japan) at 120 ℃. The digests were evaporated to dryness and re-dissolved in 7M HCl containing 0.001% H_2O_2. Each sample was split for iron concentration analysis by inductively-coupled plasma mass spectroscopy (ICP-MS; Agilent 7700) and another for isotope analysis. Iron concentrations were determined from a single aliquot of each tissue sample.

Iron purification was performed used anion-exchange chromatography following Maréchal et al., (1999). Interfering
80 elements (Ni, Cr, Cu) were removed with 7M HCl, and Fe was subsequently eluted with 2M HCl. The purified Fe fraction was dissolved in 2% HNO_3 at a concentration of 1 µg/mL, with Cu added for mass bias correction.

Stable isotope ratios were determined by multicollector-ICP-MS (Neptune Plus, ThermoFisher Scientific) at The University of Tokyo. Instrumental settings were: RF power 1200 W; Ar gas flow 15 L/min (cool), 0.7 L/min (auxiliary), 1.0 L/min (nebulizer). Signal intensity was 5–8 V for 1 µg/mL $^{56}Fe^{+}$, with blanks below 0.004 V. Each tissue sample was measured
85 once for iron isotope composition with 60 analytical cycles. The δ^{56}Fe value was expressed relative to IRMM-014 as:

$$\delta^{56}Fe = \left[\frac{(^{56}Fe/^{54}Fe)_{sample}}{(^{56}Fe/^{54}Fe)_{IRMM-014}} - 1\right] \times 1000\ [‰] \quad (3)$$

Whole-body δ^{56}Fe (δ_{WB}) was calculated as:

$$\delta_{WB} = \sum_i (\delta^{56}Fe_i \times T_i) = \sum_i (\delta^{56}Fe_i \times C_i \times M_i) \quad (4)$$

where i represent the i-th tissue, and T_i, C_i, and M_i represent the Fe burden, Fe concentration, and tissue mass, respectively.

Analytical accuracy was verified using certified reference materials (BCR-414, DORM-4, DOLT-5, ERM-CE464). Results were consistent with reported values: BCR-414 (−0.10 ± 0.03‰), DORM-4 (−0.24 ± 0.06‰), DOLT-5 (−2.32 ± 0.02‰), ERM-CE464 (−0.55 ± 0.02‰).

2.3 XANES Spectroscopy

Iron K-edge XANES was analyzed at BL-12C, Photon Factory (KEK, Japan) following the protocol of Hasegawa et al. (2023). Frozen tissue fragments were analyzed in fluorescence mode using a Si detector, with energy calibration against hematite (7110.2 eV). The number of independent spectral components was determined by principal component analysis (PCA).

The dominant Fe species in animal tissues include heme (Fe–porphyrin), ferritin (storage), and transferrin (Fe transport). Transferrin-bound Fe was excluded from further analysis due to minor abundance and negligible isotope fractionation (Walczyk and Von Blanckenburg, 2005). Thus, subsequent analyses focused on ferritin- and heme-bound Fe species. Linear combination fitting (LCF) was performed to quantify their relative proportions in each tissue.

To account for possible post-mortem oxidation of hemoproteins, spectra of oxyHb, deoxyHb, and metHb were included in the fitting. Horse spleen ferritin (Hs-Ft) and bovine blood metHb (Bb-metHb) were used as reference standards, while oxyHb and deoxyHb were prepared from metHb following Di Iorio (1981) and Wilson et al. (2013). Pre-edge features were extracted and fitted using pseudo-Voigt functions implemented in Python. The quality of spectra fits was evaluated using the R-factor, defined as:

$$R = \frac{\sum\{\chi_{obs}(E) - \chi_{cal}(E)\}^2}{\sum\{\chi_{obs}(E)\}^2} \quad (5)$$

2.4 Statistical Analysis

Statistical analyses were conducted in Python (ver. 3.9.19). Sex differences in physiological traits, Fe concentration, and isotope ratios were tested using the Mann–Whitney U test.

3 Results

3.1 Physiological Parameters of Chub Mackerel

The six chub mackerel analyzed had fork lengths (mean ± 2 S.D.) of 37.7 ± 2.41 cm in females and 40.9 ± 4.00 cm in males, and corresponding body weights of 0.71 ± 0.30 kg and 0.89 ± 0.24 kg, respectively (Table 1). Although females tended to be slightly smaller, the difference in body length was not significant ($p = 0.06$). Based on the growth curve of Shiraishi et al. (2008), all individuals were estimated to be at least four years old and sexually mature. The hepatosomatic index (HSI) ranged from 1.05–2.14 in females and 0.74–1.26 in males, and the gonadosomatic index (GSI) ranged from 4.26–10.1 in females and 7.25–10.0 in males, consistent with the spawning season in the East China Sea (Shiraishi et al., 2008). Among tissues, white muscle represented the largest biomass fraction (31–52% of total body weight; Fig. S1), followed by gonads (3.8–8.9%), red muscle (4.5–7.7%), gills (2.1–3.9%), liver (0.4–1.9%), heart (0.2–0.6%), and spleen (0.2–0.4%). No significant sex-related differences were observed ($p > 0.05$). Red and white muscles, as well as gills, exhibited strong positive correlations with body weight ($r > 0.82$, $p < 0.04$), whereas gonads showed a positive but non-significant trend ($r = 0.77$, $p = 0.07$; Fig. S2).

Table 1: Physiological parameters of chub mackerels.

	Mk-1	Mk-2	Mk-3	Mk-4	Mk-5	Mk-6	Mean
Sex	female	female	female	male	male	male	
Body weight [kg]	0.64	0.92	0.58	0.94	0.72	1	0.80
Total length [cm]	40.3	41.9	41	45.2	41.6	48.1	43.0
Fork length [cm]	37	39.4	36.7	40.8	38.5	43.4	39.3
GSI	10.1	10.1	4.26	8.76	10.0	7.25	8.41
HSI	2.14	1.48	1.05	1.07	0.74	1.06	1.26

3.2 Tissue Iron Concentrations and Stable Isotope Ratios

Mean iron concentrations (± 2 S.D.) were highest in the spleen (3,100 ± 860 μg/g d.w.), followed by blood (1,300 ± 480 μg/g d.w.), heart (720 ± 580 μg/g d.w.), liver (630 ± 510 μg/g d.w.), gills (290 ± 90 μg/g d.w.), red muscle (250 ± 84 μg/g d.w.), gonads (37 ± 24 μg/g d.w.), and white muscle (15 ± 10 μg/g d.w.) (Fig. 1A). Male spleens tended to have higher Fe concentrations than those of females, and liver and gonads also tended to be higher in males.

Assuming a blood volume of 30 mL/kg and 1.05 as the specific gravity of fish blood (Davison, 2011), the total iron content in blood was estimated to be between 3.2 and 10.3 mg (Table S1). Red muscle contributed the next largest Fe pool (2.3–6.1 mg), followed by gills (1.3–3.7 mg), white muscle (0.9–2.0 mg), spleen (0.8–2.6 mg), liver (0.5–2.0 mg), gonads (0.3–1.0 mg), and heart (0.2–0.9 mg). The total body iron inventory was therefore estimated to be approximately 17–26 mg/kg.

Although the liver is the principal iron storage tissue, it accounted for only 4–8% of total body iron. In contrast, blood and red muscle together comprised 51–67% of the total iron burden.

Mean iron isotope compositions (δ^{56}Fe ± 2 S.D.) of each tissue across individuals were as follows: red muscle, −1.54 ± 0.20‰; white muscle, −1.46 ± 0.21‰; liver, −1.19 ± 0.16‰; gonads, −1.23 ± 0.42‰; spleen, −1.37 ± 0.15‰; heart, −1.43 ± 0.19‰; gills, −1.37 ± 0.22‰; and blood, −1.39 ± 0.20‰ (Fig. 2). The net δ^{56}Fe in whole mackerel bodies weighted by tissue Fe contents ranged from −1.50‰ to −1.35‰ with the liver in all individuals showing higher values than the net values. No sex differences were detected, although ovarian δ^{56}Fe was lower than testicular values.

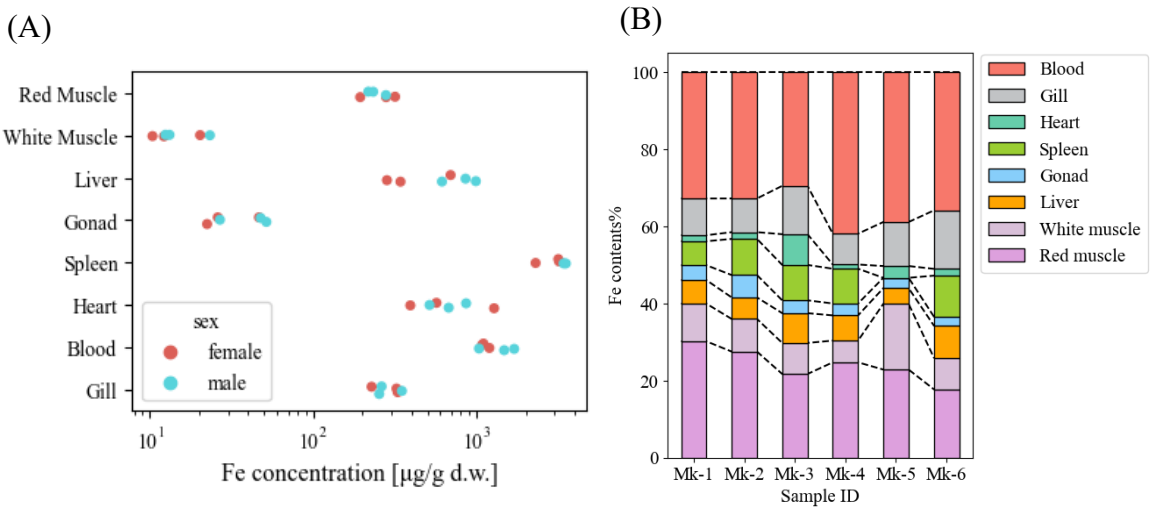

Figure 1: (A) Iron concentration, and (B) Tissue iron burden of the chub mackerels (Mk-1 to Mk-3: female, Mk-4 to Mk-6: male). Total blood contents were assumed to be 30 mL/kg with a specific gravity of 1.05. No uncertainty is reported as multiple sample replicates were not measured. The measurement uncertainty was assumed to be zero.

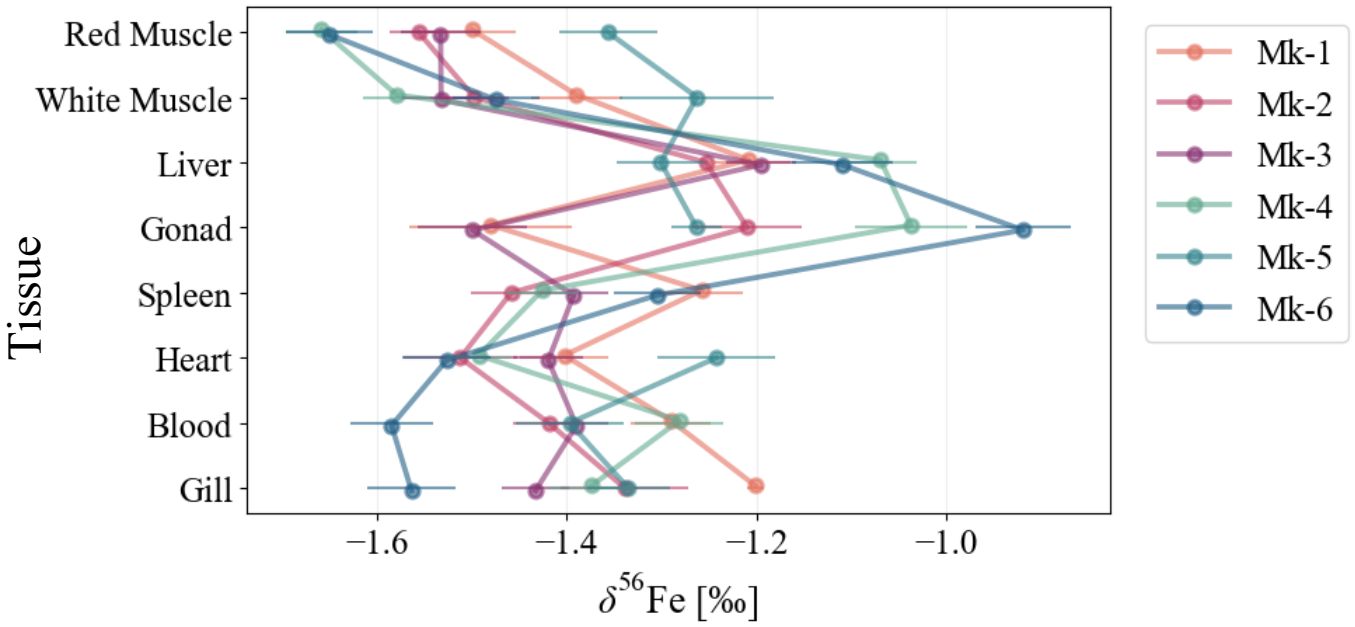

Figure 2: Iron stable isotope ratio in tissues of the six *Scomber japonicus* individuals (Mk1-3: females, Mk4-6: males). Error bars represent 2 S.E. during a single measurement (60 analytical cycles).

3.3 Proportion of Ferritin-Bound Iron

Iron K-edge XANES spectra identified the dominant chemical forms of iron in each tissue (Wilke et al., 2001). Pre-edge peak positions for all samples were distributed between ferritin (most oxidized) and hemoglobin (reduced) reference standards (Fig. 3A). We note that the XANES spectrum of MK-2 liver was unavailable because its quality was not good.

Linear combination fitting (LCF) using Hs-Ft and Bb-Hb derivatives revealed that red muscle and heart were dominated by heme-bound Fe, whereas ferritin accounted for 8–31% of total Fe in the liver (Fig. 3B). One individual exhibited extremely low liver ferritin iron (8%). The liver ferritin fraction was comparable to those reported for chub mackerel from other regions (28%; Hasegawa et al., 2023) but substantially lower than those of mouse liver (66%; Chen and Chen, 2018).

Sex-related differences were also apparent: females exhibited lower ferritin-bound Fe proportions in the liver, while higher proportions in the red muscle and gonads than males. In ovaries, ferritin represented the predominant Fe form (70–80%), whereas testes showed highly variable proportions (3–59%).

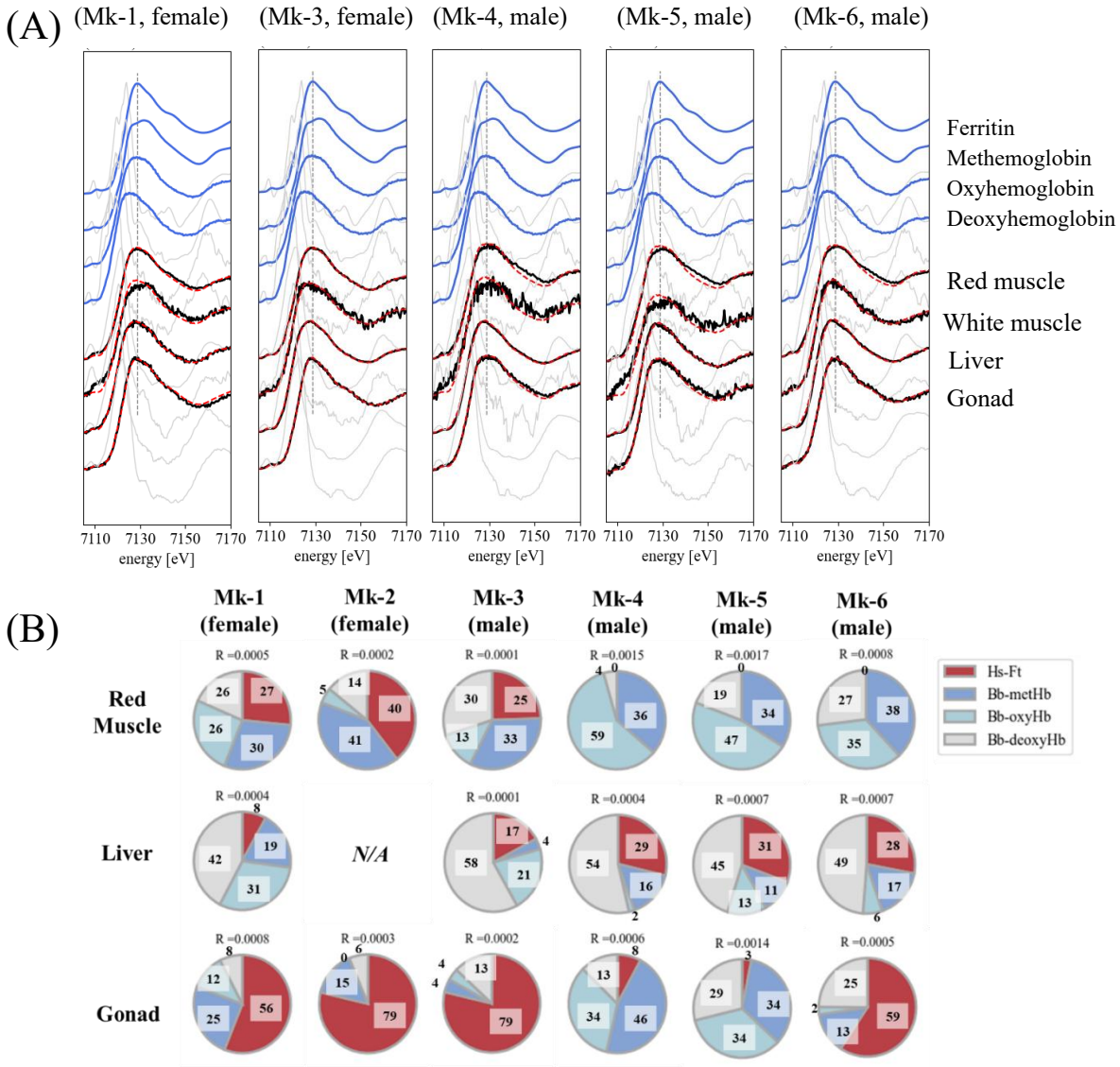

Figure 3: (A) Fe K-edge XANES spectra of *Scomber japonicus* tissues (Mk-1 and Mk-3: female, Mk-4 to Mk-6: male). Mk-1 and Mk-3 represent females, and Mk-4 to Mk-6 represent males. The standard spectra were obtained from ferritin from horse spleen and hemoglobin derivatives from bovine blood. Blue lines indicate the spectra of the standard materials, while black lines represent the tissue samples. Red dashed lines show the results of linear combination fitting (LCF) using the four standard spectra. Gray solid lines correspond to the first derivative of the normalized XANES spectra, which highlights the peak top energies, and gray dashed lines mark the peak top energy of Ferritin at 7129 eV. (B) Estimated proportions of each standard materials with linear combination fitting (LCF) of XANES spectra. R value is a goodness-of-fit parameter described in Eq. 4. Each number on the pie charts represents proportions (%) of each component.

4 Discussion

4.1 Elevated δ^{56}Fe in Liver and Contribution of Ferritin-Bound Iron

First, we focused on the liver because it is a central tissue for iron storage in vertebrates and is expected to exhibit iron isotope fractionation through the synthesis of ferritin. All the chub mackerel individuals showed higher δ^{56}Fe values in the liver than δ_{WB} across eight tissues. Because ferritin preferentially incorporates heavier Fe isotopes during the oxidation in the storage process according to human studies (Albarède et al., 2011), this enrichment most likely reflects the contribution of ferritin-bound iron within the liver. It should be noted that human ferritin consists of H and L subunits responsible for iron oxidation and mineralization (Plays et al., 2021). While teleost ferritin includes an additional M-type subunit with intermediate functional properties, its effect on iron oxidation and isotope fractionation remains unclear and is not considered further here (Dickey et al., 1987; Andersen et al., 1995).

The proportion of ferritin-bound Fe in mackerel liver (8–31%) was notably lower than that reported for mammalian liver (~60%; Chakrabarti et al., 2015; Chen and Chen, 2018), suggesting that a smaller fraction of hepatic Fe is stored as ferritin in teleost. Consequently, the δ^{56}Fe enrichment in the mackerel liver appears more moderate than in mammals, possibly due to a greater influence of isotopically lighter Fe pools such as circulating hemoglobin iron.

Because blood contains little ferritin-bound iron, the elevated liver δ^{56}Fe cannot be explained by residual blood contamination. Given that iron cycling within the body is a semi-closed system, in which the liver acts as the central exchange site between storage (ferritin) and transport (hemoglobin and transferrin) pools (Slusarczyk and Mleczko-Sanecka, 2021), hepatic δ^{56}Fe can be interpreted as a mixture of these isotopically distinct components. This relationship can be expressed as:

$$\delta_{Liv} = p\delta_{Ft} + (1-p)\,\delta_{Hm} \quad (6)$$

where p is the fraction of ferritin-bound Fe in the liver, and δ_{Ft} and δ_{Hm} represent the isotopic compositions of ferritin- and heme-bound Fe, respectively.

By assuming that the lowest δ^{56}Fe observed here in red muscle represents δ_{Hm} (-1.66‰), the isotopic offset between ferritin- and heme-bound Fe in the liver ($\Delta = \delta_{Ft} - \delta_{Hm}$) was estimated to be 2.72 ± 3.03‰ (2 S.D.) in all specimens, whereas 4.15 ± 2.84‰ (2 S.D.) in females and 1.76 ± 0.88‰ in males. These estimated values are higher than previous observations in skipjack tuna (*Katsuwonus pelamis*, female, Δ = 1.52‰, n = 1; Hasegawa et al., 2023) and another chub mackerel specimen (Δ = 1.41‰, male, n = 1; Hasegawa et al., 2023), and, in females, appear higher than the equilibrium isotope fractionation between Fe(II) and Fe(III) (~2.8‰、Johnson et al., 2002; Welch et al., 2003). The two females exhibited a lower ferritin-bound iron fraction than the three males, while their liver δ^{56}Fe values are comparable to those of the males, resulting in a tendency for their estimated Δ values to be higher. Because of the limited sample size, it cannot be definitively concluded that a sex difference exists. However, one possible explanation is that the release of isotopically lighter Fe from hepatic ferritin following Rayleigh fractionation leads to significant enrichment of heavy Fe in the residual ferritin and results in Δ values

larger than those expected under isotopic equilibrium. As the sample consists of mature individuals during the spawning season, it cannot be ruled out that physiological changes relating to spawning may have temporarily altered iron metabolism, particularly in females.

4.2 δ^{56}Fe Variation Across Tissues

Outside the liver, some tissues did not exhibit elevated δ^{56}Fe values despite high ferritin content. In particular, ovaries and red muscle in females exhibited high ferritin-to-heme ratios but δ^{56}Fe values comparable to other tissues. This pattern suggests that ferritin-bound Fe in these tissues is not retained over long periods but is actively mobilized and recycled in response to metabolic activity and oxygen consumption. For example, ferritin in skeletal muscle can be quickly mobilized to meet oxygen demand (Robach et al., 2007; Ryan et al., 2021), preventing the accumulation of a heavy isotope signature and maintaining δ^{56}Fe values close to those of the whole-body iron pool dominated by heme iron. Moreover, δ^{56}Fe has been associated with oxidative stress markers including superoxide dismutase and glutathione peroxidase (Sauzéat et al., 2025), indicating that tissues prone to oxidative stress, such as gonads, may display isotopic variability due to redox-related iron turnover.

These observations suggest that ferritin-bound (storage) iron in chub mackerel exhibits a high turnover rate, resulting in small δ^{56}Fe differences among tissues. In contrast, heme iron likely turns over more slowly. Fish erythrocyte lifespans range from ~80 to 500 days (Götting and Nikinmaa, 2017; Avery et al., 1992), comparable or longer than those of mice (~60 days, Dholakia et al., 2015) and humans (~120 days; Shemin and Rittenberg, 1946). Marine mammals, by contrast, display extended erythrocyte lifespans that scale with diving capacity (Pearson et al., 2024), highlighting the link between oxygen storage and iron utilization. In migratory fish such as mackerel, the high and continuous demand for heme to support aerobic activity may promote rapid redistribution of heme iron, which may result in reduced δ^{56}Fe variability among organs.

4.3 Features of δ^{56}Fe Variation Among Marine Species

The range of δ^{56}Fe variation among tissues in chub mackerel was clearly narrower than that reported for mammals. For example, the differences in δ^{56}Fe values between muscle and liver range from 0.72‰ to 1.71‰ in mice (Balter et al., 2013), 1.64‰ to 2.72‰ in sheep (Balter et al., 2013), and 0.83‰ to 1.75‰ in humans (Walczyk and von Blanckenburg, 2002), whereas the maximum isotopic difference among tissues in the present chub mackerel specimens was 0.73‰. Despite this relatively small internal fractionation, δ^{56}Fe values in marine organisms often show species-specific ranges (Figure 4). For example, muscular δ^{56}Fe values in skipjack tuna are high regardless of regional differences (−1.46‰ to −0.71‰; Hasegawa et al., 2022), whereas mammals generally show lower values (−3.79‰ to −1.5‰; Walczyk and von Blanckenburg, 2002; Balter et al., 2013). This pattern does not appear to arise from the enrichment of lighter isotopes in specific tissues, but rather

from the limited influence of internal isotopic fractionation on whole-body δ^{56}Fe. This interpretation is consistent with our previous study on a single individual (Hasegawa et al., 2023), and the limited inter-tissue δ^{56}Fe variation observed across multiple individuals in the present work supports that this characteristic is generally applicable to chub mackerel.

As discussed in the previous section, hepatic ferritin iron likely undergoes isotopic fractionation on the order of approximately 1.5–3‰, based on the Δ values estimated in this study and Hasegawa et al. (2023). However, because ferritin constitutes only a small fraction of total iron, its contribution to whole-body δ^{56}Fe variation is limited. Consequently, heterogeneous distribution of δ^{56}Fe across tissues is likely to have only a minor influence on the δ^{56}Fe of indicator tissues representing whole-body δ^{56}Fe values (e.g. muscle with a large Fe pool size). The primary determinant of tissue δ^{56}Fe in chub mackerel therefore appears to be iron uptake process from external sources rather than internal redistribution.

The relatively high mean δ^{56}Fe values in mackerel tissues may primarily reflect more efficient intestinal iron absorption than in mammals, resulting in a stronger reflection of environmental δ^{56}Fe values. Additionally, selective ingestion of prey with intrinsically higher δ^{56}Fe values could also contribute to their isotopic composition. Various prey taxa of marine fish, including zooplankton, squid, and crustaceans, are known to exhibit relatively high δ^{56}Fe values (−1.00‰ to −0.03‰; von Blanckenburg et al., 2013; Hasegawa et al., 2022, 2023). The δ^{56}Fe differences observed among fish groups such as tuna and mackerel (−1.58‰ to −0.71‰) versus sardine and herring (−2.64‰ to −1.73‰; Hasegawa et al., 2022) seemed difficult to explain solely by isotopic differences in their prey since all prey species analyzed so far showed higher δ^{56}Fe values than sardine and herring (Hasegawa et al., 2022). However, recent studies have suggested species-specific δ^{56}Fe variability even among zooplankton (Hasegawa et al., submitted) and therefore prey-derived δ^{56}Fe may also partially contribute to the overall isotopic composition of fish such as sardines and herrings that feed selectively on specific plankton groups. Further expansion of marine biological δ^{56}Fe databases may enable a more comprehensive understanding of Fe physiology in wild marine organisms.

In contrast, terrestrial mammals such as humans, mice, and sheep consistently show large δ^{56}Fe differences between liver and muscle (Walczyk and von Blanckenburg, 2002; Balter et al., 2013), reflecting a well-developed iron recycling system based on the long-term ferritin storage. This mechanism reduces daily iron requirements and promotes preferential uptake of lighter isotopes, thereby lowering the overall δ^{56}Fe values. In contrast to mammals that rely on ferritin-based iron storage and recycling, the isotopic pattern observed in fish may indicate that long-term iron storage plays a less dominant role in iron homeostasis, despite inhabiting chronically iron-limited environments. They may instead have evolved a "recycle dominant" mode of iron homeostasis that relies on intensive recycling of iron to sustain metabolic demands.

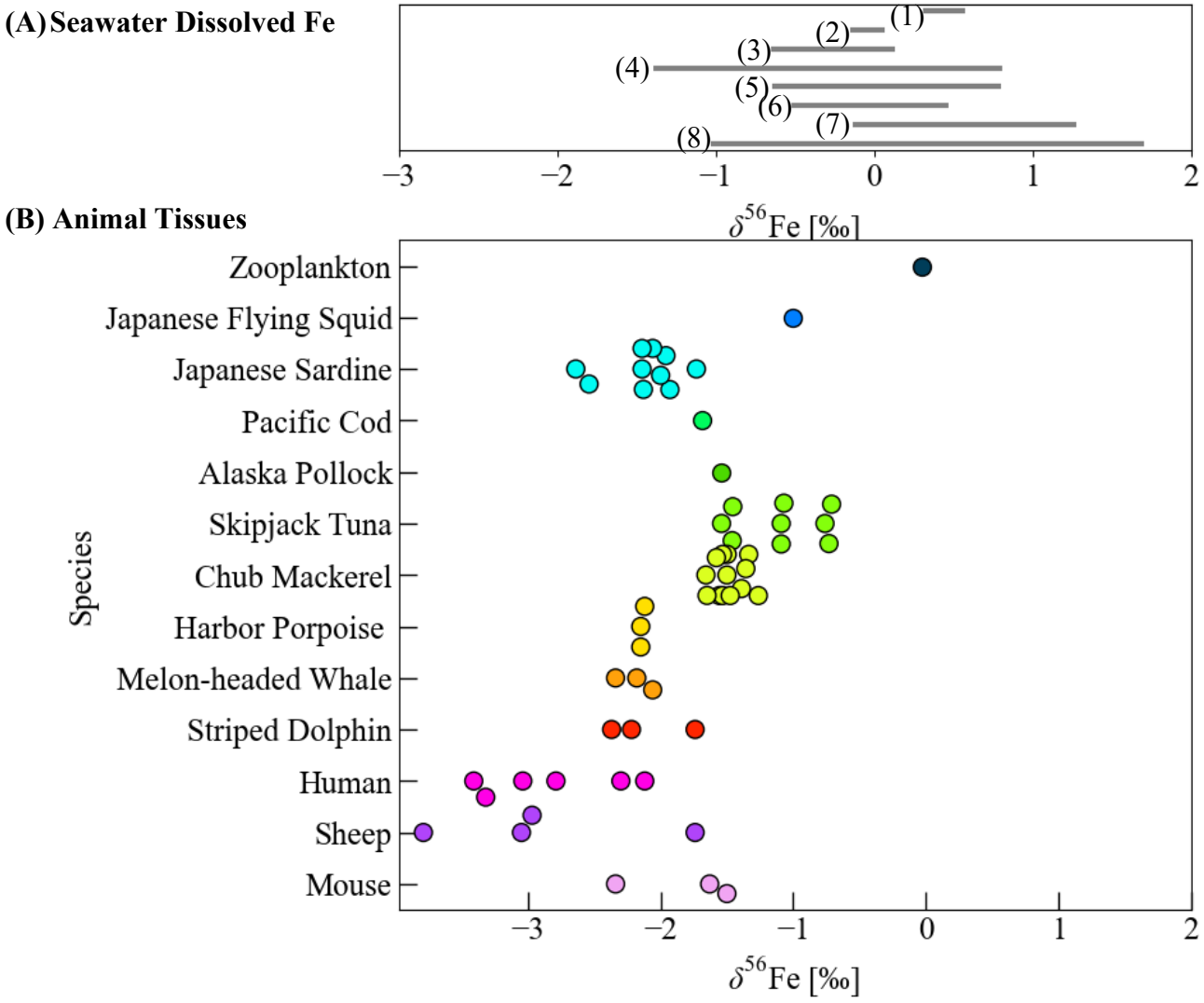

Figure 4: Comparison of δ^{56}Fe values in seawater (upper figure), and marine organisms and mammals (lower figure). Literature data in the upper figure are indicated by reference numbers: seawater from the Pacific Ocean (1–4: Radic et al., 2011; Conway and John, 2015; Pinedo-González et al., 2020; Kurisu et al., 2024), North Atlantic Ocean (5: Conway and John, 2014), and South Atlantic–Southern Ocean (6–8: Abadie et al., 2017; Ellwood et al., 2020; Sieber et al., 2021). The data of chub mackerel includes this study and Hasegawa et al. (2023), while values for zooplankton (whole body), squid (mantle), and mammals (harbor porpoise, melon-headed whale, striped dolphin, human, sheep, and mouse) are compiled from previous studies (Walczyk and von Blanckenburg, 2002; Balter et al., 2013; Hasegawa et al., 2022).

4.4 Implications for biological iron cycling in marine environments

The results of this study suggest that the δ^{56}Fe variability in marine fish reflects dietary characteristics and uptake efficiency more strongly than internal physiological variations. The distinctly lighter isotopic signatures of animals compared to seawater may ultimately influence the isotopic composition of iron recycled through marine food webs. Therefore, whole-body δ^{56}Fe values could serve as an integrated tracer of biologically available iron within marine ecosystems. Our analyses also indicate that in fish, δ^{56}Fe values in non-destructive tissues such as blood can represent the whole-body isotopic composition, highlighting their potential as key species for assessing iron supply and cycling in higher marine ecosystems.

In the future, applying a Rayleigh-type model may allow quantitative evaluation of the relative contributions of absorption and retention to isotopic fractionation in fish. Combined with XAFS analyses that provide species-level insights into ferritin- and heme-bound iron pools, these approaches could offer a powerful framework for linking biological iron metabolism to marine biogeochemical iron cycling. In addition, further biochemical studies examining Fe isotope fractionation during enzymatic incorporation into iron-binding proteins such as ferritin or heme in fish would help to better constrain the mechanisms controlling Fe isotope distribution in marine organisms.

5 Conclusions

This study demonstrates that δ^{56}Fe variations among tissues in chub mackerel are smaller than those observed in mammals. Although isotopic fractionation of around 1.5-3‰ may occur in liver ferritin, its effect on whole-body δ^{56}Fe is minimal due to the limited ferritin fraction and overall liver iron content. These results suggest that the high δ^{56}Fe of mackerel primarily reflects dietary iron sources and intestinal uptake rather than internal isotopic fractionation. The maximum δ^{56}Fe range among major tissues was 0.73‰, indicating relatively small tissue isotopic variability. The small variation in δ^{56}Fe among major tissues such as muscle and liver compared with the potential isotopic fractionation associated with ferritin formation, suggests that iron isotope pools in fish remain relatively stable. Although the number of individuals analysed in this study is limited, these δ^{56}Fe patterns across multiple individuals provide robust constraints on iron isotope behaviour in wild marine fish. These findings provide fundamental information for studies of iron cycling and metabolism in marine organisms and have potential applications in food-web modeling and ecological assessments.

Supplement

This manuscript includes a supplementary material.

Author contribution

NH and TI contributed conceptualization, Methodology, and Project Administration; NH conducted Formal analysis, Software, Investigation, Visualization, and Writing (original draft preparation); YT and TI contributed Writing (review and editing); NH, YT and TI contributed Funding Acquisition.

Data availability

The data underlying this study are available in the article itself and its supplementary material.

Competing interests

The authors declare that they have no conflict of interest.

Acknowledgement

The authors appreciate Mr. Kei Zenimoto and Prof. Kotaro Shirai for collecting and transporting mackerel samples. We also thank Mr. Kotaro Hirayama and Mr. Yuma Sato for helping with the dissection of fish samples. We used ChatGPT to improve the English clarity and readability of the manuscript. This work was performed under the approval of the Photon Factory Program Advisory Committee (Proposal No. 2023G119, 2023S2-001, and 2022G126). This work was supported by JST SPRING, Grant Number JPMJSP2108, and Asahi Group Foundation Grant Number A24-0057.

References

Abadie, C., Lacan, F., Radic, A., Pradoux, C., Poitrasson., F.: Iron isotopes reveal distinct dissolved iron sources and pathways in the intermediate versus deep Southern Ocean. Proc. Natl. Acad. Sci. USA, 114: 858–863, doi: 10.1073/pnas.1603107114, 2017.

Albalat, E., Cavey, T., Leroyer, P., Ropert, M., Balter, V., and Loréal, O.: Hfe Gene Knock-Out in a Mouse Model of Hereditary Hemochromatosis Affects Bodily Iron Isotope Compositions, Front. Med., 8, 711822, doi: 10.3389/fmed.2021.711822, 2021.

Albarède, F., Telouk, P., Lamboux, A., Jaouen, K., and Balter, V.: Isotopic evidence of unaccounted for Fe and Cu erythropoietic pathways, Metallomics, 3, 926–933, doi: 10.1039/c1mt00025j, 2011.

Allaya, H., Hattour, A., Hajjej, G., and Trabelsi, M.: Biologic characteristics of Scomber japonicus (Houttuyn , 1782) in Tunisian waters (Central Mediterranean Sea), Afr. J. Biotechnol., 12, 3040, doi: 10.5897/AJB12.2723, 2013.

Andersen, O., Dehli, A., Standal, H., Giskegjerde, T. A., Karstensen, R., Rørvik, K. A.: Two ferritin subunits of Atlantic salmon (Salmo salar): cloning of the liver cDNAs and antibody preparation.Mol. Mar. Biol. Biotechnol., 4, 164-170, 1995.

Boyd, P. W., Watson, A. J., Law, C. S., Abraham, E. R., Trull, T., Murdoch, R., Bakker, D. C. E., Bowie, A. R., Buesseler, K. O., Chang, H., Charette, M., Croot, P., Downing, K., Frew, R., Gall, M., Hadfield, M., Hall, J., Harvey, M., Jameson, G., Laroche, J., Liddicoat, M., Ling, R., Maldonado, M. T., Mckay, R. M., Nodder, S., Pickmere, S., Pridmore, R., Rintoul, S., Safi, K., Sutton, P., Strzepek, R., Tanneberger, K., Turner, S., Waite, A., and Zeldis, J.: A mesoscale phytoplankton bloom in the polar Southern Ocean stimulated by iron fertilization, Nature, 407, 695–702, doi: 10.1038/35037500, 2000.

Brill, R. W., Cousins, K. L., Jones, D. R., Bushnell, P. G., and Steffensen, J. F.: Blood volume, plasma volume and circulation time in a high-energy-demand teleost, the yellowfin tuna (*Thunnus albacares*), J. Exp. Biol., 201, 647–654, doi: 10.1242/jeb.201.5.647, 1998.

Bury, N. R., Grosell, M., Wood, C. M., Hogstrand, C., Wilson, R. W., Rankin, J. C., Busk, M., Lecklin, T., and Jensen, F. B.: Intestinal iron uptake in the European flounder (*Platichthys flesus*), J. Exp. Biol., 204, 3779–3787, doi: 10.1242/jeb.204.21.3779, 2001.

Carriquiriborde, P., Handy, R. D., and Davies, S. J.: Physiological modulation of iron metabolism in rainbow trout (*Oncorhynchus mykiss*) fed low and high iron diets, J. Exp. Biol., 207, 75–86, doi: 10.1242/jeb.00712, 2004.

Chakrabarti, M., Cockrell, A. L., Park, J., McCormick, S. P., Lindahl, L. S., and Lindahl, P. A.: Speciation of iron in mouse liver during development, iron deficiency, IRP2 deletion and inflammatory hepatitis, Metallomics, 7, 93–101, doi: 10.1039/c4mt00215f, 2015.

Chen, R. and Chen, G.: Tumor-induced disorder of iron metabolism in major organs: A new insight from chemical speciation of iron, J. Int. Med. Res., 46, 70–78, doi: 10.1177/0300060517718711, 2018.

Conway, T. M., John, S. G.: Quantification of Dissolved Iron Sources to the North Atlantic Ocean. Nature, 511, 212–215, doi: 10.1038/nature13482, 2014.

Conway, T. M., John, S. G.: The Cycling of Iron, Zinc and Cadmium in the North East Pacific Ocean - Insights from Stable Isotopes. Geochim. Cosmochim. Acta, 164, 262–283. doi: 10.1016/j.gca.2015.05.023, 2015.

Crichton, R. R. and Boelaert, J. R.: Inorganic biochemistry of iron metabolism : from molecular mechanisms to clinical consequences, John Wiley & Sons, 2001.

Davison, P.: The specific gravity of mesopelagic fish from the northeastern Pacific Ocean and its implications for acoustic backscatter. *ICES J. Mar. Sci.*, 68, 2064-2074, doi: 10.1093/icesjms/fsr140, 2011.

Dholakia, U., Bandyopadhyay, S., Hod, E. A., and Prestia, K. A.: Determination of RBC survival in C57BL/6 and C57BL/6-Tg (UBC–GFP) mice. Comp. Med., *65*, 196–201, 2015.

Dickey, L. F., Sreedharan, S., Theil, E. C., Didsbury, J. R., Wang, Y. H., Kaufman, R. E.: Differences in the regulation of messenger RNA for housekeeping and specialized-cell ferritin. A comparison of three distinct ferritin complementary DNAs, the corresponding subunits, and identification of the first processed in amphibia. J. Biol. Chem., *262*, 7901-7907, doi: 10.1016/S0021-9258(18)47653-3, 1987.

Di Iorio, E. E.: Preparation of derivatives of ferrous and ferric hemoglobin, Methods Enzymol., 76, 57–72, doi: 10.1016/0076-6879(81)76114-7, 1981.

Ellwood, M. J., Strzepek, R. F., Strutton, P. G., Trull, T. W., Fourquez, M., Boyd., P. W.: Distinct iron cycling in a Southern Ocean eddy. Nat. Comm. 11, 825, doi: 10.1038/s41467-020-14464-0, 2020.

Fiorito, V., Crich, S. G., Silengo, L., Altruda, F., Aime, S., and Tolosano, E.: Assessment of iron absorption in mice by ICP-MS measurements of ^{57}Fe levels, Eur. J. Nutr., 51, 783–789, doi: 10.1007/s00394-011-0256-6, 2012.

Flórez, M. R., Anoshkina, Y., Costas-Rodríguez, M., Grootaert, C., Van Camp, J., Delanghe, J., and Vanhaecke, F.: Natural Fe isotope fractionation in an intestinal Caco-2 cell line model, J. Anal. At. Spectrom., 32, 1713–1720, doi: 10.1039/c7ja00090a, 2017.

Galbraith, E. D., Mézo, P. Le, Hernandez, G. S., Bianchi, D., and Kroodsma, D.: Growth limitation of marine fish by low iron availability in the open ocean, Front. Mar. Sci., 6, 509, doi: 10.3389/fmars.2019.00509, 2019.

Georgiadis, M. M., Komiya, H., Chakrabarti, P., Woo, D., Kornuc, J. J., and Rees, D. C.: Crystallographic Structure of the Nitrogenase Iron Protein from *Azotobacter vinelandii*, Science, 257, 1653–1659, doi: 10.1126/science.1529353, 1992.

Hasegawa, N., Itai, T., Kunisue, T., and Takahashi, Y.: Variation of Iron Stable Isotopes in a Marine Ecosystem from the Northwest Pacific Ocean, Chem. Lett., 51, 556–560, doi: 10.1246/cl.220099, 2022.

Hasegawa, N., Takahashi, Y., and Itai, T.: Tissue-variation of iron stable isotopes in marine fish coupled with speciation analysis using X-ray absorption fine structure, Sci. Total Environ., 881, 163449, doi: 10.1016/j.scitotenv.2023.163449, 2023.

Hatta, M., Measures, C. I., Wu, J., Roshan, S., Fitzsimmons, J. N., Sedwick, P., and Morton, P.: An overview of dissolved Fe and Mn distributions during the 2010-2011 U.S. GEOTRACES north Atlantic cruises: GEOTRACES GA03, Deep Sea Res. 2 Top. Stud. Oceanogr., 116, 117–129, doi: 10.1016/j.dsr2.2014.07.005, 2015.

Hoffbrand, A. V., Ganeshaguru, K., Hooton, J. W. L., and Tattersall, M. H. N.: Effect of Iron Deficiency and Desferrioxamine on DNA Synthesis in Human Cells, Br. J. Haematol., 33, 517–526, doi: 10.1111/j.1365-2141.1976.tb03570.x, 1976.

Hotz, K. and Walczyk, T.: Natural iron isotopic composition of blood is an indicator of dietary iron absorption efficiency in humans, J. Biol. Inorg. Chem., 18, 1–7, doi: 10.1007/s00775-012-0943-7, 2013.

Hotz, K., Krayenbuehl, P. A., and Walczyk, T.: Mobilization of storage iron is reflected in the iron isotopic composition of blood in humans, J. Biol. Inorg. Chem., 17, 301–309, doi: 10.1007/s00775-011-0851-2, 2012.

Itazawa, Y., Takeda, T., Yamamoto, K., and Azuma, T.: Determination of Circulating Blood Volume in Three Teleosts,Carp,Yellowtail and Porgy, Jpn. J. Ichthyol. 30, 94–101, doi: 10.11369/jji1950.30.94, 1983.

Jaouen, K. and Balter, V.: Menopause effect on blood Fe and Cu isotope compositions, Am. J. Phys. Anthropol., 153, 280–285, doi: 10.1002/ajpa.22430, 2014.

Johnson, C. M., Skulan, J. L., Beard, B. L., Sun, H., Nealson, K. H., and Braterman, P. S.: Isotopic fractionation between Fe (III) and Fe (II) in aqueous solutions, *Earth Planet. Sci. Lett.*, 195, 141-153, doi: 10.1016/S0012-821X(01)00581-7, 2002.

Johnson, K. S., Gordon, R. M., and Coale, K. H.: What controls dissolved iron concentrations in the world ocean?, Mar. Chem., 57, 137–161, doi: 10.1016/S0304-4203(97)00043-1, 1997.

Kurisu, M., Sakata, K., Nishioka, J., Obata, H., Conway, T. M., Hunt, H. R., Sieber, M., Suzuki, K., Kashiwabara, T., Kubo, S., Takada, M., Takahashi, Y.: Source and Fate of Atmospheric Iron Supplied to the Subarctic North Pacific Traced by Stable Iron Isotope Ratios. Geochim. Cosmochim. Acta, 378, 168–185. doi: 10.1016/j.gca.2024.06.009, 2024.

Krayenbuehl, P. A., Walczyk, T., Schoenberg, R., von Blanckenburg, F., and Schulthess, G.: Hereditary hemochromatosis is reflected in the iron isotope composition of blood, Blood, 105, 3812–3816, doi: 10.1182/blood-2004-07-2807, 2005.

Kwong, R. W. M. and Niyogi, S.: An in vitro examination of intestinal iron absorption in a freshwater teleost, rainbow trout (*Oncorhynchus mykiss*), J. Comp. Physiol. B, 178, 963–975, doi: 10.1007/s00360-008-0279-3, 2008.

Maréchal, C. N., Télouk, P., and Albarède, F.: Precise analysis of copper and zinc isotopic compositions by plasma-source mass spectrometry, Chem. Geol., 156, 251–273, doi: 10.1016/S0009-2541(98)00191-0, 1999.

Martin, J. H. and Gordon, R. M.: Northeast Pacific iron distributions in relation to phytoplankton productivity, Deep-Sea Res. Pt.A Oceano. Res. Pap., 35, 177–196, doi: 10.1016/0198-0149(88)90035-0, 1988.

Martin, J. H., Gordon, R. M., Fitzwater, S., and Broenkow, W. W.: VERTEX: phytoplankton/iron studies in the Gulf of Alaska, Deep-Sea Res. Pt.A Oceano. Res. Pap., 36, 649-680, doi:10.1016/0198-0149(89)90144-1, 1989.

Nishioka, J. and Obata, H.: Dissolved iron distribution in the western and central subarctic Pacific: HNLC water formation and biogeochemical processes, Limnol. Oceanogr., 62, 2004–2022, doi: 10.1002/lno.10548, 2017.

Plays, M., Müller, S., Rodriguez, R.: Chemistry and biology of ferritin, Metallomics, *13*, mfab021, doi: 10.1093/mtomcs/mfab021, 2021.

Radic, A., Lacan, F., Murray, J. W.: Iron isotopes in the seawater of the equatorial Pacific Ocean: New constraints for the oceanic iron cycle. *Earth Planet. Sci. Lett.*, *306*, 1-10, doi: 10.1016/j.epsl.2011.03.015, 2011

Pinedo-González, P., Hawco, N. J., Bundy, R. M.: Anthropogenic Asian aerosols provide Fe to the North Pacific Ocean. Proc. Natl. Acad. Sci. USA, 117, 27862–27868, doi: 10.1073/pnas.2010315117, 2020.

Robach, P., Cairo, G., Gelfi, C., Bernuzzi, F., Pilegaard, H., Viganò, A., Santambrogio, P., Cerretelli, P., Calbet, J. A. L., Phane Moutereau, S., and Lundby, C.: Strong iron demand during hypoxia-induced erythropoiesis is associated with down-regulation of iron-related proteins and myoglobin in human skeletal muscle, Blood, 109, 4724–4731, doi: 10.1182/blood-2006-08-040006, 2007.

Robbins, E. and Pederson, T.: Iron: its intracellular localization and possible role in cell division., Proc. Natl. Acad. Sci., 66, 1244–1251, doi: 10.1073/pnas.66.4.1244, 1970.

Ryan, B. J., Foug, K. L., Gioscia-Ryan, R. A., Varshney, P., Ludzki, A. C., Ahn, C., Schleh, M. W., Gillen, J. B., Chenevert, T. L., and Horowitz, J. F.: Exercise training decreases whole-body and tissue iron storage in adults with obesity, Exp. Physiol., 106, 820–827, doi: 10.1113/EP089272, 2021.

Sauzéat, L., Moreira, M., Holota, H., Beaudoin, C., and Volle, D. H.: Unveiling the hidden impact of long-term metal-rich volcanic pollution on male reproductive functions using isotope metallomics, Environ. Int., 198, 109388, doi: 10.1016/j.envint.2025.109388, 2025.

Shemin, D., and Rittenberg, D.: The life span of the human red blood cell. J.Biol. Chem., 166, 627–636, 1946.

Shiraishi, T., Okamoto, K., Yoneda, M., Sakai, T., Ohshimo, S., Onoe, S., Yamaguchi, A., and Matsuyama, M.: Age validation, growth and annual reproductive cycle of chub mackerel *Scomber japonicus* off the waters of northern Kyushu and in the East China Sea, Fish. Sci., 74, 947–954, doi: 10.1111/j.1444-2906.2008.01612.x, 2008.

Slusarczyk, P. and Mleczko-Sanecka, K.: The multiple facets of iron recycling, Genes, 12, 1364, doi: 10.3390/genes12091364, 2021.

Sieber, M., Conway, T. M., de Souza, G. F., Hassler, C. S., Ellwood, M. J., Vance. D.: Isotopic fingerprinting of biogeochemical processes and iron sources in the iron-limited surface Southern Ocean. Earth Planet. Sci. Lett., 567. 116967. doi: 10.1016/j.epsl.2021.116967, 2021.

Stenberg, A., Malinovsky, D., Rodushkin, I., Andrén, H., Pontér, C., Öhlander, B., and Baxter, D. C.: Separation of Fe from whole blood matrix for precise isotopic ratio measurements by MC-ICP-MS: A comparison of different approaches, J. Anal. At. Spectrom., 18, 23–28, doi: 10.1039/b210482b, 2003.

von Blanckenburg, F., Noordmann, J., and Guelke-Stelling, M.: The iron stable isotope fingerprint of the human diet, J. Agric. Food Chem., 61, 11893–11899, doi: 10.1021/jf402358n, 2013.

van den Heuvel, E. G., Muys, T., Pellegrom, H., Bruyntjes, J. P., Van Dokkum, W., Spanhaak, S., and Schaafsma, G.: A new method to measure iron absorption from the enrichment of ^{57}Fe and ^{58}Fe in young erythroid cells. *Clinical chemistry*, *44*, 649–654, doi: 10.1093/clinchem/44.3.649,1998.

van Heghe, L., Delanghe, J., Van Vlierberghe, H., and Vanhaecke, F.: The relationship between the iron isotopic composition of human whole blood and iron status parameters, Metallomics, 5, 1503–1509, doi: 10.1039/c3mt00054k, 2013.

van Heghe, L., Deltombe, O., Delanghe, J., Depypere, H., and Vanhaecke, F.: The influence of menstrual blood loss and age on the isotopic composition of Cu, Fe and Zn in human whole blood, J. Anal. At. Spectrom., 29, 478–482, doi: 10.1039/c3ja50269d, 2014.

von Blanckenburg, F., Noordmann, J., and Guelke-Stelling, M.: The iron stable isotope fingerprint of the human diet, J. Agric. Food Chem., 61, 11893–11899, doi: 10.1021/jf402358n, 2013.

Walczyk, T. and Von Blanckenburg, F.: Deciphering the iron isotope message of the human body, Int. J. Mass Spectrom., 242, 117–134, doi: 10.1016/j.ijms.2004.12.028, 2005.

Welch, S. A., Beard, B. L., Johnson, C. M., and Braterman, P. S.: Kinetic and equilibrium Fe isotope fractionation between aqueous Fe (II) and Fe (III). *Geochim. Cosmochim. Acta*, *67*, 4231-4250, doi: 10.1016/S0016-7037(03)00266-7, 2003.

Wilke, M., Farges, F., Petit, P. E., Brown, G. E., and Martin, F.: Oxidation state and coordination of Fe in minerals: An Fe K-XANES spectroscopic study, American Mineralogist, 86, 714–730, doi: 10.2138/am-2001-5-612, 2001.

Wilson, S. A., Green, E., Mathews, I. I., Benfatto, M., Hodgson, K. O., Hedman, B., and Sarangi, R.: X-ray absorption spectroscopic investigation of the electronic structure differences in solution and crystalline oxyhemoglobin, Proc. Natl. Acad. Sci., 110, 16333–16338, doi: 10.1073/pnas.1315734110, 2013.